Volume 6 No.4 - February 22 2016
www.small-journal.com

small

NANO MICRO

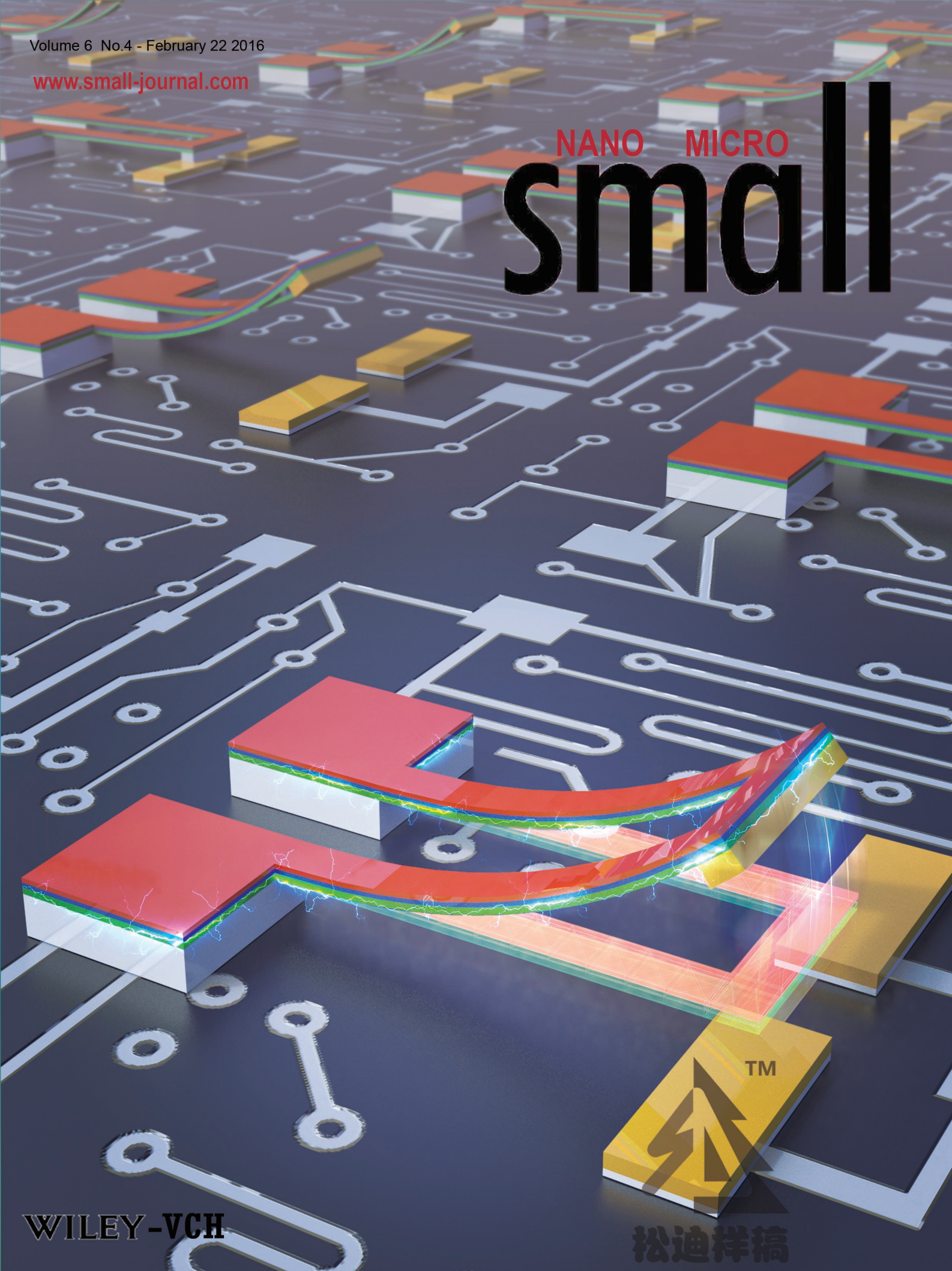

WILEY-VCH

small
www.small-journal.com

A 0.2 V Micro-Electromechanical Switch Enabled by a Phase Transition

Kaichen Dong, Hwan Sung Choe, Xi Wang, Huili Liu, Bivas Saha, Changhyun Ko, Yang Deng, Kyle B. Tom, Shuai Lou, Letian Wang, Costas P. Grigoropoulos, Zheng You, Jie Yao,* and Junqiao Wu**

Micro-electromechanical (MEM) switches, with advantages such as quasi-zero leakage current, emerge as attractive candidates for overcoming the physical limits of complementary metal-oxide semiconductor (CMOS) devices. To practically integrate MEM switches into CMOS circuits, two major challenges must be addressed: sub 1 V operating voltage to match the voltage levels in current circuit systems and being able to deliver at least millions of operating cycles. However, existing sub 1 V mechanical switches are mostly subject to significant body bias and/or limited lifetimes, thus failing to meet both limitations simultaneously. Here 0.2 V MEM switching devices with $\gtrsim 10^6$ safe operating cycles in ambient air are reported, which achieve the lowest operating voltage in mechanical switches without body bias reported to date. The ultralow operating voltage is mainly enabled by the abrupt phase transition of nanolayered vanadium dioxide (VO_2) slightly above room temperature. The phase-transition MEM switches open possibilities for sub 1 V hybrid integrated devices/circuits/systems, as well as ultralow power consumption sensors for Internet of Things applications.

Dr. K. Dong, Dr. H. S. Choe, Dr. X. Wang, Dr. H. Liu, Dr. B. Saha, Prof. C. Ko, Y. Deng, K. B. Tom, S. Lou, Prof. J. Yao, Prof. J. Wu
Department of Materials Science and Engineering
University of California
Berkeley, CA 94720, USA
E-mail: yaojie@berkeley.edu; wuj@berkeley.edu

Dr. K. Dong, Dr. H. S. Choe, Dr. H. Liu, Dr. B. Saha, Prof. C. Ko, K. B. Tom, Prof. J. Yao, Prof. J. Wu
Materials Sciences Division
Lawrence Berkeley National Laboratory
Berkeley, CA 94720, USA

Dr. K. Dong, Prof. Z. You
State Key Laboratory of Precision Measurement Technology and Instruments
Department of Precision Instrument
Tsinghua University
Beijing 100084, P. R. China
E-mail: yz-dpi@mail.tsinghua.edu.cn

L. Wang, Prof. C. P. Grigoropoulos
Department of Mechanical Engineering
University of California
Berkeley, CA 94720, USA

The ORCID identification number(s) for the author(s) of this article can be found under https://doi.org/10.1002/smll.201703621.

DOI: 10.1002/smll.201703621

The silicon industry is always demanding better performance and lower power consumption in complementary metal-oxide semiconductor (CMOS)-based systems for new applications, such as the Internet of Things[1] and smart dusts.[2] Therefore, mechanical switches thrive as an attractive alternative to CMOS devices that suffer from their inevitable limitations, mostly leakage currents.[3–7] The application of micro-electromechanical (MEM) switches promises considerable advances in logic inverters,[8] sensors,[9] communication systems,[10] etc. However, to integrate MEM switches into current systems, the challenge of matching their operating voltages with the CMOS levels (<1 V) with good reliability must be addressed.[3,5,7,11–14] Research efforts so far have been focused on lowering the operating voltages by either improving the device design or reducing the device size.[3,15,16] A body bias method has also been introduced to reduce the gate voltage, but it fails to decrease the overall operating voltage because the body bias voltage is usually high (≈4–12 V).[4,17–19] Currently, sub 1 V switches without body bias are mostly based on nano-electromechanical (NEM) technologies using ultrasmall air gaps or ultrathin piezoelectric layers.[3,15] However, the reported operating cycles of those sub 1 V switches are mostly limited to $<10^2$, which presents a critical obstacle to their practical application.[3,13,14]

On the other hand, attributes of VO_2 promise a favorable role in the MEM switch field. First, VO_2 undergoes a rapid, thermally driven phase transition from the insulating (I) to the metallic (M) phase when heated above the transition temperature (T_c = 68 °C),[20–23] which results in a large and abrupt lattice change (strain) to actuate the switch. Second, the in-plane strain of VO_2 across the phase transition is 1% or 0.3% in single-crystal samples or polycrystal films, respectively, with volumetric work densities comparable to those of shape memory alloys (SMA) and much larger than those of thermal expansion and piezoelectric materials.[22] As such, the reversible phase transition of VO_2 assures high actuation/restoring force output, resulting in a good electrode–electrode contact and a low chance of irreversible stiction.[5,24] Third, unlike SMA, VO_2 has little or no ductility, and is able to work with a relatively narrow

hysteretic loop at nanoscale thicknesses,[22,23,25,26] thus having the potential to be integrated into MEM switches for optimized switching time and power consumption. Indeed, using conventional microfabrication processes/facilities, VO_2-based bimorph microactuators have been demonstrated with $\gtrsim 10^6$ operating cycles or ≳kHz switching frequencies.[22,23,27] Consequently, the phase-transition material of VO_2 is potentially an effective solution to solve the two major problems of operating voltage and lifetime in MEM switches.[7]

Despite these encouraging attributes of VO_2, research to implement VO_2 MEM devices is still far from maturity. The main barriers lie in the uncontrolled and nonflat initial curvatures of the VO_2 bimorphs, as well as the chemical vulnerability of VO_2 in the fabrication process. The former obstacle has recently been tackled with a "seesaw" method to balance the initial strains.[28] Based on this method, we present the first VO_2 phase-transition MEM switch fabricated on a single chip, with ≈0.2 V operating voltages, $\gtrsim 10^6$ operating cycles, and potential applications such as an ultralow power consumption temperature alarm.

As illustrated in **Figure 1**, the phase-transition MEM switch is composed of a U-shaped cantilever and two bottom electrodes. Detailed fabrication procedures are summarized in the Supporting Information. The U-shaped cantilever is a 170 µm long Au/Cr/VO_2 sandwich structure with a 75 nm thick Pt film (moving electrode) attached to the bottom of the cantilever tip. The cantilever width (W) and gap (G) are 10 and 20 µm, respectively. Similarly, the bottom electrodes are 7 nm thick Cr adhesion layers and 50 nm thick Pt electrodes patterned on top of ≈250 nm thick thermal oxide. The bottom electrodes are separated by a 10 µm gap. The anchor and bottom electrodes are large enough to prevent peel-off during the removal of the sacrificial material, as well as creating enough space for measurements in a probe station.

To perform proper switching, the initial (before the VO_2 phase transition) and final (after the transition) cantilever curvatures must be carefully controlled. The "seesaw" method,[28] which utilizes the residual stresses in all involved films for delicate stress compensation and curvature control, was used in the design, resulting in the required thicknesses of Au, Cr, and VO_2 layers to be 95, 36, and 160 nm, respectively. With such a design, at room temperature (when the VO_2 is in the I phase), the cantilever slightly bends upward, so the switch is at the OFF state with an air gap between the moving and the bottom electrodes. Upon heating above T_c, the active VO_2 layer in the cantilever transforms into the M phase with an in-plane shrinkage, driving the cantilever to bend downward until the moving electrode forms contact with the bottom electrodes. The switch is then closed (ON state).

Scanning electron microscopy (SEM) and optical images (**Figures 2**a and 2b, respectively) show the phase-transition MEM switches with configurations following the above design. To test the temperature response, global heating was first used to control the switch (Figure 2b). When the temperature of the environment changed, the phase transition of the VO_2 film actuated the cantilever and switched the ON/OFF state. Example responses of the MEM switch are depicted in Figure 2c: a 50 mV square wave at 5 Hz and 50% duty was applied to an anchor electrode as the input, while the output was measured at a bottom electrode. When the VO_2 was in the I phase, the U-shaped cantilever was bent upward and the input signal could not be transmitted to the output port. When the environment temperature was increased, the cantilever was bent down, due to a transition of VO_2 from the I phase to the M phase, and placed the electrodes in contact, allowing the output signal to accurately follow the input with an electrode contact resistance of 1×10^2 Ω.

To characterize the environment temperature-dependent behavior of the phase-transition switch, two switching modes were tested in the experiment: anchor–bottom switching (mode A) and bottom–bottom switching (mode B). In mode A, a 50 mV input signal was applied at one of the anchor electrodes, and the output was measured at one of the bottom electrodes as a function of the environment temperature (Figure 2d). When the environment temperature increased, the device showed an abrupt switching from 64 °C (OFF state) to 65 °C (ON state). As the device was cooled down, the ON-to-OFF transition occurred between 53 and 54 °C. In mode B, the input signal was applied to the other bottom electrode, and a similar hysteretic output was observed (Figure 2e). These characteristics can be explained by the phase-transition hysteresis of VO_2 as detailed in the Supporting Information.

To demonstrate the potential of the phase-transition MEM switch, we utilize the switch as a temperature alarm to highlight its abrupt and reversible response to the environment temperature. Conventional sensors usually present a burden for power budgets of some extremely low-power systems,[29] and a low inquiring frequency or a sleeping mode is generally utilized to decrease the overall power consumption at the cost of limited performance.[30] In contrast, the phase-transition MEM switch can act as an "always-ON" temperature alarm for the threshold temperature

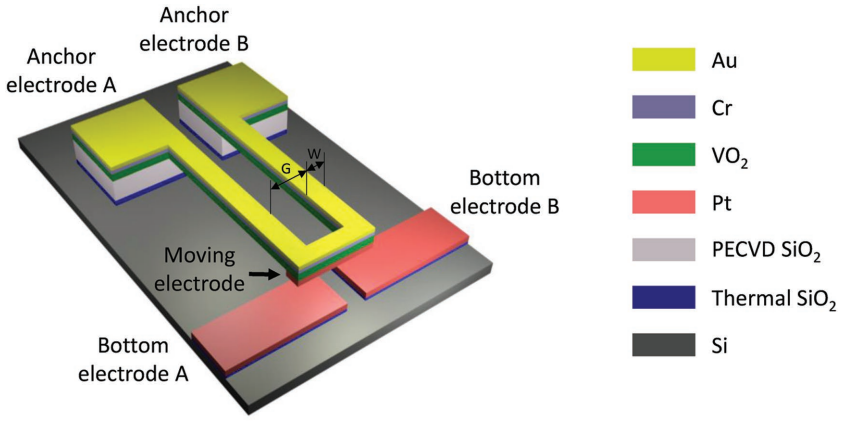

Figure 1. Schematic illustration of a phase-transition MEM switch. When the VO_2 layer is heated above its transition temperature, it undergoes a reversible phase transition and abruptly shrinks. Thus, the U-shaped cantilever is actuated by the in-plane shrinkage of VO_2, and bends downward to close the gap between the moving electrode and the bottom electrodes. Detailed configuration of the U-shaped cantilever can be found in Figure 4b.

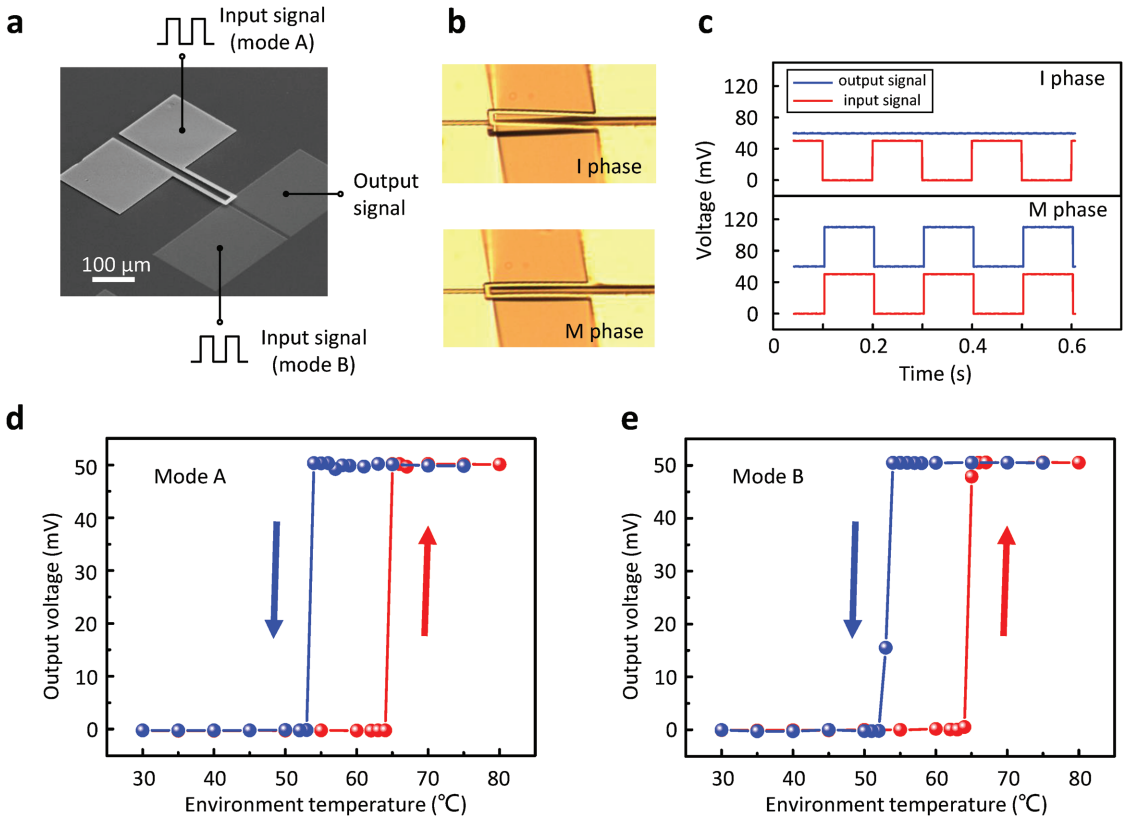

Figure 2. Switch control with environment temperature variation. a) Schematic diagram of the experimental configuration based on the SEM image of the phase-transition MEM switch. b) Optical microscopic images of the switch when VO_2 was in the I phase (OFF) or the M phase (ON). c) Examples of input and output signals of the switch when VO_2 was in the I phase or in the M phase. The output signals are vertically offset by +60 mV for clarity. d,e) The hysteretic output voltage measured at one of the bottom electrodes as a function of the environment temperature while 50 mV input was applied to d) an anchor electrode in mode A or e) the other bottom electrode in mode B.

with ultralow power consumption. This nearly ideal performance is attributed to the quasi-zero leakage current of MEM switches at the OFF state,[31] as well as the solely environment temperature-driven operation of the device in this work. Theoretically, continuous temperature monitoring can be achieved with minimum power consumption, which is promising in low-power integrated systems or wireless nodes. Here, we define the sensitivity of the temperature alarm as the minimum temperature variation that is needed to drive the switching. From Figure 2d,e, the sensitivity of the VO_2 switch is about 1 °C for mode A, and 2 °C for mode B, sufficient for various applications such as on-board overheating prevention[32] or fire alarms.[33] Moreover, such a phase-transition MEM switch is able to function as an ultralow-power temperature switch to control circuits in temperature-sensitive systems. We also note that doping VO_2 with other metals (such as tungsten[27] and chromium[34,35]) can effectively and continuously reduce or increase its T_c, hence covering a wide range of operation temperatures.

The phase-transition MEM switch can also be controlled by electrical signals, which was demonstrated by the experiment configuration in **Figure 3**a. Note that the substrate was kept at room temperature in the experiment. A square wave with 50% duty was applied to an anchor electrode, resulting in Joule heating caused by the periodic current flowing in the U-shaped cantilever. Note that only the Joule heating of the U-shaped cantilever heated up the switch for actuation. The operating voltage (V_a) applied to the switch is calculated by the input voltage (V_i) and the involved resistances in the testing circuit using Equation (1)

$$V_a = \frac{R_{s1} + R_{s2}}{R_1 + R_{s1} + R_{s2} + R_2} \times V_i \quad (1)$$

The output current as a function of V_i and V_a is depicted in Figure 3b. It can be seen that only 0.2 V is necessary to heat up the VO_2 for a phase transition and turn on the switch, which is the lowest operating voltage (without body bias) in all existing MEM/NEM switches so far. The corresponding 3 kΩ ON resistance and the over 1×10^6 ON/OFF ratio warrant superior performance of the phase-transition MEM switch. The power consumption of the device is calculated to be ≈3 mW.

The dynamic switching characterization was conducted at 1 kHz, as shown in Figure 3c, and the switch-on time was measured to be ≈150 µs, resulting in switch-on energy consumption of 450 nJ. The output voltage at the bottom electrode was close to half of the input voltage V_i due to the symmetry of the switch. Two factors contribute to the ultralow operating voltage, low power consumption, and fast response (compared to conventional Joule heating MEM switches): the low phase-transition temperature of VO_2 and the low resistance of the Au/Cr heater.

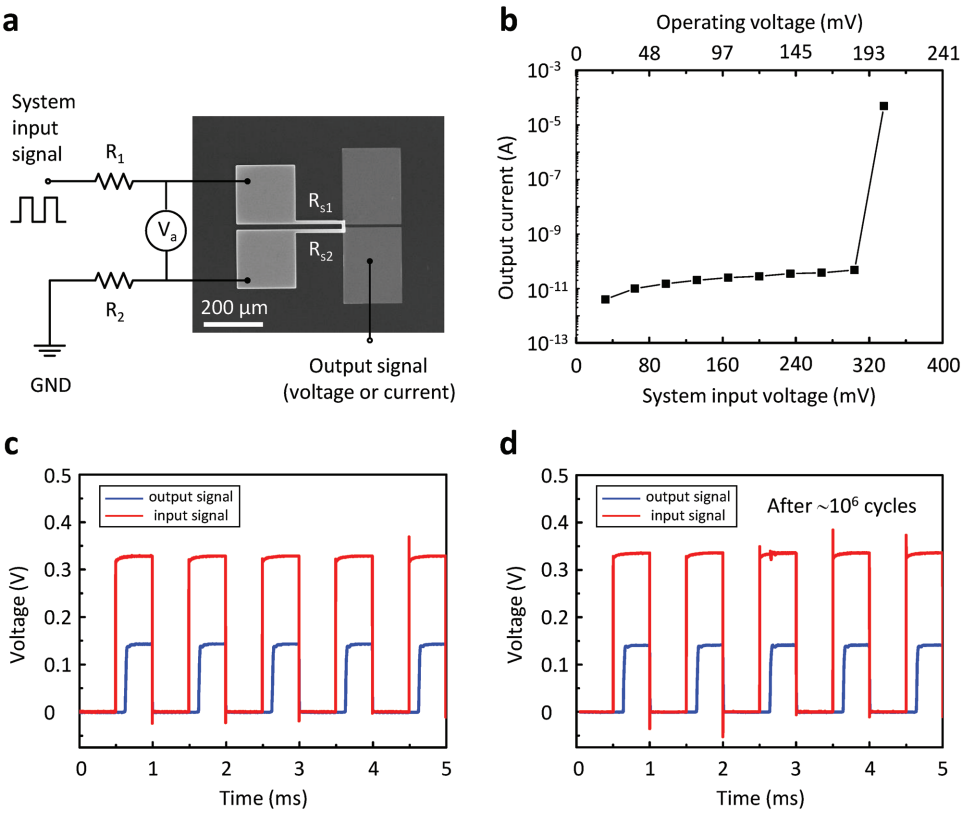

Figure 3. Switch control with Joule heating at room temperature. a) Schematic diagram of the experimental configuration. System input signal was applied to one of the anchor electrodes, providing functional current flowing through the U-shaped cantilever for Joule heating. V_i is the amplitude of the system input signal. When the VO_2 switch is turned on, the output voltages at both the bottom electrodes are proportional to the system input voltage. R_1 and R_2 denote the overall parasitic impedances introduced by the testing platform at the two anchor electrodes. R_{s1} and R_{s2} are the resistances of the U-shaped cantilever divided at the electrode–electrode contact position. V_a is the real operating voltage applied to the U-shaped cantilever ($R_{s1} + R_{s2}$). b) Measured output current as a function of the system input voltage, showing an operating voltage of 0.2 V and an ON/OFF ratio of $\approx 10^6$. Note that the operating voltage is calculated from the system input voltage and the resistances in panel (a). c) Typical ON/OFF switching experiment result conducted at 1 kHz. d) Output voltage at 1 kHz input after $\approx 10^6$ ON/OFF cycles in ambient air with no degradation observed.

To assess the reliability of the switch, endurance tests were conducted under repeated cyclic measurements in ambient air and the result is shown in Figure 3d. After $\approx 10^6$ ON/OFF cycles, the switching performance remains almost the same. Such a lifetime is enough for practical applications,[13,14] and similar conclusions have been reported in other VO_2 actuator works.[23,27] These reliability tests confirmed the mechanical and the thermal stability of VO_2 as an actuation material.

The phase-transition MEM switch is also simulated using COMSOL Multiphysics. For simplicity, a 2D model was used to simulate half of the U-shaped cantilever (**Figure 4**a) with mechanical and electrical boundary conditions illustrated in Figure 4b (see the "Experimental Section" for details). Note that the applied voltage was $0.5 \times V_a$ and the Au resistivity was modified to match the measured cantilever resistance. The simulation used parameters consistent with experimental results and the measured VO_2 resistance–temperature curves. The simulation showed that, with a 0.14 V operating voltage, a time delay of 145 µs is needed for the Pt tip to contact the bottom electrodes (Figure 4c), which is consistent with the experimental switch-on time shown in Figure 3c. If V_a is equal to the experimental operating voltage (0.2 V), the contact will form within only 65 µs. Furthermore, the antimechanical shock performance of the switch was estimated by numerical calculation as well, which proved that the switch is able to sustain up to 1800 g before it is acceleratively bent down to cause a mistaken switch-on.

In conclusion, we have demonstrated a VO_2-based phase-transition MEM switch with ≈0.2 V operating voltages and $\gtrsim 10^6$ life cycles. The device was also used to demonstrate an ultralow power consumption temperature alarm/switch. The integration of the phase-transition material VO_2 into MEM switches brings unique merits. First, the switching performance benefits from the low T_c of VO_2, as well as the abrupt change in its structure during the phase transition. Second, VO_2 responds well to diverse external stimuli (e.g., temperature, electrical current, and light), which would transduce other types of energy into the actuation, and realize electrothermally or photothermally controlled switches. Third, the phase-transition temperature of VO_2 can be engineered by doping, defects, stoichiometry, and microstructures, creating abundant design space. For example, the performance of the VO_2-based MEM switch can be further improved by W-doping for lower T_c,[27] and Cr-doping may increase T_c to allow the phase-transition MEM switch to operate at temperatures as high as +85 °C.[34,35] Downscaling the device size with NEM technology can significantly reduce power

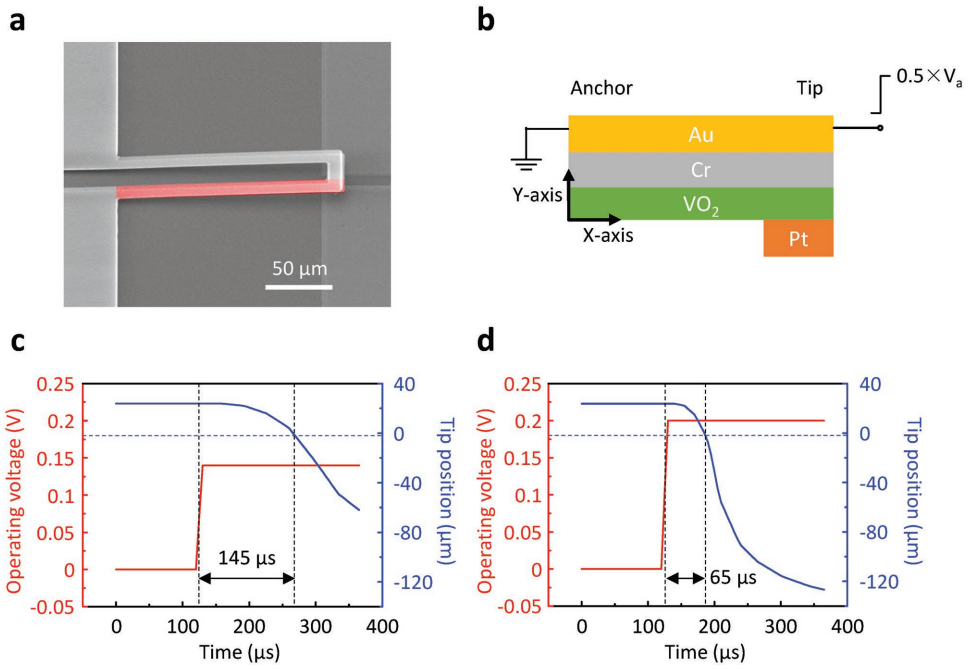

Figure 4. Numerical simulation. a) A false-colored SEM image of the switch showing the simulated part. b) Schematic of the 2D simulation of the phase-transition MEM switch. Note that the blocks are not drawn to the scale, and the applied voltage at the tip is only half of the operating voltage. c,d) Time-dependent tip displacement when c) 0.14 V or d) 0.2 V operating voltage is applied. The horizontal blue dashed lines indicate the position of the bottom electrodes.

consumption as well as switch-on time (see the Supporting Information), and better electrode–electrode contact can be attained by optimizing the fabrication process and device configuration for higher contact force and lower contact resistance. Aided with mature microfabrication technologies, the phase-transition MEM switches would open possibilities of sub 1 V hybrid integrated devices/circuits/systems and ultralow power consumption devices for practical applications.

Experimental Section

VO_2 Growth: Polycrystalline VO_2 films were grown on plasma-enhanced chemical-vapor-deposited SiO_2 by pulsed laser deposition (PLD). A krypton fluoride excimer laser (λ = 248 nm) and a VO_2 target (99%) were used for the PLD. The fluence and repetition rate of the pulsed laser were 320 mJ and 5 Hz, respectively. The oxygen pressure was 5 mTorr, and the substrate temperature was kept at 575 °C during the VO_2 deposition.

Phase-Transition MEM Switch Characterization: The global heating and cooling were controlled with a Lakeshore 321 temperature controller and a home-made heating stage, which was composed of two Kapton insulated flexible heaters, one Pt temperature sensor and a copper heat sink. The characterization experiments were carried out with a Cascade Microtech M150 probe station. Other facilities involved in the characterization included a Stanford Research Systems SR570 low-noise current preamplifier for output current measurement, an Agilent 33220A 20 MHz function/arbitrary waveform generator for square wave generation or voltage supplement, and a Keysight InfiniiVision DSO-X 2024A oscilloscope for recording both the input and output signals.

Phase-Transition MEM Switch Simulation: As shown in Figure 4b, the 2D phase-transition MEM switch model was an Au/Cr/VO_2 trilayered cantilever with a Pt electrode attached to the tip. The geometric sizes of the blocks matched the real VO_2 switch design.

The model included three coupled physics: solid mechanics, heat transfer in solids, and electric currents. The left boundary of the cantilever was mechanically fixed while all the other boundaries were free. The anchor boundary was assigned a constant temperature of 20 °C to simulate the good thermal dissipation through the anchor to the substrate. Other boundaries had convective heat transfer with the surroundings, so a natural convention boundary condition was applied. To accurately calculate the necessary operating voltage to actuate the cantilever, the cantilever resistance was adjusted to match the experimental data. The electrical potential of the cantilever tip was set to be 0.5 × V_a, while the anchor boundary was electrically grounded.

The mechanical properties (e.g., residual stress, density, Young's modulus, and Poisson's ratio) were adopted from previous reports as well as our measured results.[28] In order to simulate the phase transition of the polycrystalline VO_2 film, temperature-dependent electrical conductivity, thermal conductivity, and effective internal stress of the VO_2 film were obtained by combining the above parameters in the I phase and the M phase with the measured VO_2 resistance–temperature curve.[20,28,36] The latent heat of the VO_2 phase transition was integrated into the temperature-dependent heat capacity of VO_2.[37]

Supporting Information

Supporting Information is available from the Wiley Online Library or from the author.

Acknowledgements

This work was supported by the Center for Energy Efficient Electronics Science (NSF Award No. 0939514). K.D. acknowledges the China Scholarship Council (CSC, Grant No. 201406210211) for financial support. Partial measurement and fabrication were done in the U.C. Berkeley Marvell Nanolab and Biomolecular Nanotechnology Center.

The authors are grateful to Prof. K. Liu, Prof. Y. Ruan, Prof. J. Zhao, Prof. Z. Hou, Prof. P. Dong, J. W. Beeman, Y. Chen, B. Ma, Y. Gao, P. Ci, H. Zhu, Z. Gong, X. Lei, K. Chen, K. Wang, M. Hettick, Y. Liu, and E. Cardona for helpful discussions.

Conflict of Interest

The authors declare no conflict of interest.

Keywords

Micro-electromechanical systems, phase transitions, sub 1 V operating voltages, switch, vanadium dioxide

Received: October 17, 2017
Revised: December 6, 2017
Published online: February 26, 2018

[1] D. Miorandia, S. Sicarib, F. De Pellegrinia, I. Chlamtac, *Ad Hoc Networks* **2012**, *10*, 1497.
[2] J. M. Kahn, R. H. Katz, K. S. J. Pister, in *Proc. of ACM/IEEE Intl. Conf. on Mobile Computing and Networking (MOBICOM)*, ACM, New York, NY **1999**, pp. 271–278.
[3] J. O. Lee, Y.-H. Song, M.-W. Kim, M.-H. Kang, J.-S. Oh, H.-H. Yang, J.-B. Yoon, *Nat. Nanotechnol.* **2013**, *8*, 36.
[4] B. Osoba, B. Saha, L. Dougherty, J. Edgington, C. Qian, F. Niroui, J. H. Lang, V. Bulović, J. Wu, T.-J. K. Liu, in *IEEE IEDM*, IEEE, San Francisco, CA, USA **2016**, p. 655.
[5] O. Y. Loh, H. D. Espinosa, *Nat. Nanotechnol.* **2012**, *7*, 283.
[6] K. Roy, S. Mukhopadhyay, H. Mahmoodi-Meimand, *Proc. IEEE* **2003**, *91*, 305.
[7] J.-B. Yoon, Y.-H. Yoon, M.-H. Seo, S.-D. Ko, Y.-H. Song, M.-W. Kim, H.-H. Yang, J. O. Lee, W.-W. Jang, in *19th Int. Conf. on Solid-State Sensors, Actuators and Microsystems (TRANSDUCERS)*, IEEE, Kaohsiung, Taiwan **2017**, p. 171.
[8] Y.-H. Song, S.-J. K. Ahn, M.-W. Kim, J.-O. Lee, C.-S. Hwang, J.-E. Pi, S.-D. Ko, K.-W. Choi, S.-H. K. Park, J.-B. Yoon, *Small* **2015**, *11*, 1390.
[9] W. Zhu, C. S. Wallace, Y. Zhang, N. Yazdi, in *18th Int. Conf. on Solid-State Sensors, Actuators and Microsystems (TRANSDUCERS)*, IEEE, Anchorage, AK, USA **2015**, p. 556.
[10] E. Pirmoradi, H. Mirzajani, H. B. Ghavifekr, *Microsyst. Technol.* **2015**, *21*, 465.
[11] S. Xu, Y. Qin, C. Xu, Y. Wei, R. Yang, Z. L. Wang, *Nat. Nanotechnol.* **2010**, *5*, 366.
[12] B. Tian, X. Zheng, T. J. Kempa, Y. Fang, N. Yu, G. Yu, J. Huang, C. M. Lieber, *Nature* **2007**, *449*, 885.
[13] M. C. Scardelletti, C. A. Zorman, D. R. Oldham, in *IEEE Int. Symp. Antennas and Propagation Society*, IEEE, San Diego, CA, USA **2008**, p. 1.
[14] R. J. Parroa, M. C. Scardellettib, N. C. Varaljayb, S. Zimmermanc, C. A. Zorman, *Solid-State Electron.* **2008**, *52*, 1647.
[15] U. Zaghloul, G. Piazza, *IEEE Electron Device Lett.* **2014**, *35*, 669.
[16] Y. Qian, B. W. Soon, C. Lee, *J. Microelectromech. Syst.* **2015**, *24*, 1878.
[17] H.-H. Yang, D.-H. Choi, J. O. Lee, J.-B. Yoon, in *IEEE MEMS Conf.* IEEE, Wanchai, Hong Kong, China **2010**, p. 747.
[18] N. Sinha, T. S. Jones, Z. Guo, G. Piazza, *J. Microelectromech. Syst.* **2012**, *21*, 484.
[19] I.-R. Chen, L. Hutin, C. Park, R. Lee, R. Nathanael, J. Yaung, J. Jeon, T.-J. K. Liu, *ECS Trans.* **2012**, *45*, 101.
[20] D. Fu, K. Liu, T. Tao, K. Lo, C. Cheng, B. Liu, R. Zhang, H. A. Bechtel, J. Wu, *J. Appl. Phys.* **2013**, *113*, 043707.
[21] A. Cavalleri, C. Tóth, C. W. Siders, J. A. Squier, F. Ráksi, P. Forget, J. C. Kieffer, *Phys. Rev. Lett.* **2001**, *87*, 237401.
[22] K. Liu, C. Cheng, Z. Cheng, K. Wang, R. Ramesh, J. Wu, *Nano Lett.* **2012**, *12*, 6302.
[23] K. Liu, C. Cheng, J. Suh, R. Tang-Kong, D. Fu, S. Lee, J. Zhou, L. O. Chua, J. Wu, *Adv. Mater.* **2014**, *26*, 1746.
[24] N. Tas, T. Sonnenberg, H. Jansen, R. Legtenberg, M. Elwenspoek, *J. Micromech. Microeng.* **1996**, *6*, 385.
[25] A. Rúa, F. E. Fernández, N. Sepúlveda, *J. Appl. Phys.* **2010**, *107*, 074506.
[26] R. Cabrera, E. Merced, N. Sepúlveda, *J. Microelectromech. Syst.* **2014**, *23*, 243.
[27] H. Ma, J. Hou, X. Wang, J. Zhang, Z. Yuan, L. Xiao, Y. Wei, S. Fan, K. Jiang, K. Liu, *Nano Lett.* **2017**, *17*, 421.
[28] K. Dong, S. Lou, H. S. Choe, K. Liu, Z. You, J. Yao, J. Wu, *Appl. Phys. Lett.* **2016**, *109*, 023504.
[29] S. Jeong, Z. Foo, Y. Lee, J.-Y. Sim, D. Blaauw, D. Sylvester, *IEEE J. Solid-State Circuits* **2014**, *49*, 1682.
[30] B. Warneke, M. Last, B. Liebowitz, K. S. J. Pister, *Computer* **2001**, *34*, 44.
[31] Y.-H. Yoon, Y.-H. Song, S.-D. Ko, C.-H. Han, G.-S. Yun, M.-H. Seo, J.-B. Yoon, *J. Microelectromech. Syst.* **2016**, *25*, 217.
[32] V. Szekely, C. Marta, Z. Kohari, M. Rencz, *IEEE Trans. Very Large Scale Integration (VLSI) Syst.* **1997**, *5*, 270.
[33] J. Lloret, M. Garcia, D. Bri, S. Sendra, *Sensors* **2009**, *9*, 8722.
[34] K. Miyazaki, K. Shibuya, M. Suzuki, H. Wado, A. Sawa, *Jpn. J. Appl. Phys.* **2014**, *53*, 071102.
[35] A. Rúa, R. Cabrera, H. Coy, E. Merced, N. Sepúlveda, F. E. Fernández, *J. Appl. Phys.* **2012**, *111*, 104502.
[36] J. H. Park, J. M. Coy, T. S. Kasirga, C. Huang, Z. Fei, S. Hunter, D. H. Cobden, *Nature* **2013**, *500*, 431.
[37] X. Zhong, X. Zhang, A. Gupta, P. LeClair, *J. Appl. Phys.* **2011**, *110*, 084516.

